

4.1. X-RAY DIFFRACTION (XRD) - MATERIAL CHARACTERIZATION

4.1.1. X-ray Diffraction Analysis (XRD)

X-ray diffraction (XRD) measurements were made for PVC. The XRD pattern shows the nature of crystallinity with respect to PVC. PVC is a semi-crystalline polymer with peaks at  $2\theta$  angles  $17.3^\circ$  and  $18.2^\circ$ , typical of a polymer which is partially crystalline. Figure 4.1 and 4.2 shows the XRD patterns of PVC. The XRD pattern of PVC shows peaks at  $2\theta$  angles  $17.3^\circ$ ,  $18.2^\circ$  and  $20.4^\circ$ . The XRD pattern of PVC shows peaks at  $2\theta$  angles  $17.3^\circ$ ,  $18.2^\circ$  and  $20.4^\circ$ . These peaks are characteristic of PVC.

# Chapter 4

## Results & Discussion II



Figure 4.1. XRD pattern of PVC.

## 4.0 RESULTS AND DISCUSSION II - MATERIAL CHARACTERIZATION

### 4.1 X-ray Diffraction Analysis (XRD)

X-ray diffraction (XRD) measurements were made for PVC based polymer electrolyte films to examine the nature of crystallinity with respect to pure PVC and to study the occurrence of complexation.

Figure 4.1 illustrates the x-ray diffractogram of pure PVC. It can be observed that the sample is partially crystalline with peaks at  $2\theta$  angles  $13.3^\circ$  and  $16.2^\circ$ , typical of polymers. Figure 4.2 and 4.3 shows the x-ray diffractogram of  $\text{LiCF}_3\text{SO}_3$  and  $\text{LiBF}_4$  salts.  $\text{LiCF}_3\text{SO}_3$  has sharp peaks at  $2\theta$  angles  $19.1^\circ$ ,  $22.1^\circ$  and  $32.4^\circ$  whereas  $\text{LiBF}_4$  has sharp peaks at  $2\theta$  angles  $25.8^\circ$ ,  $39.5^\circ$  and  $44.4^\circ$ . These salts are crystalline in nature.

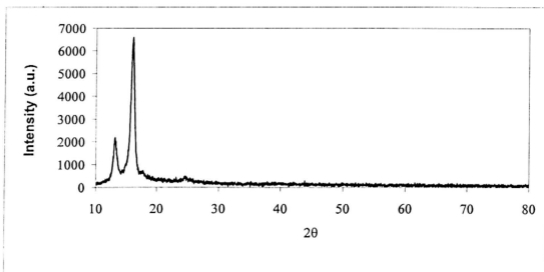
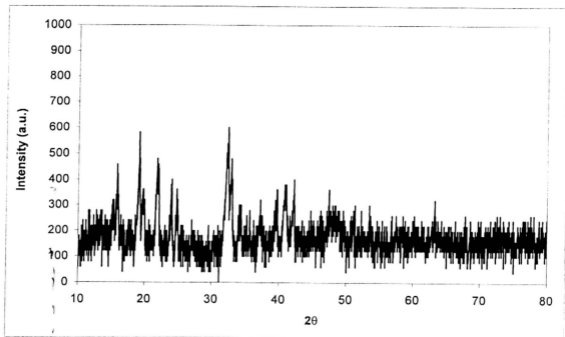
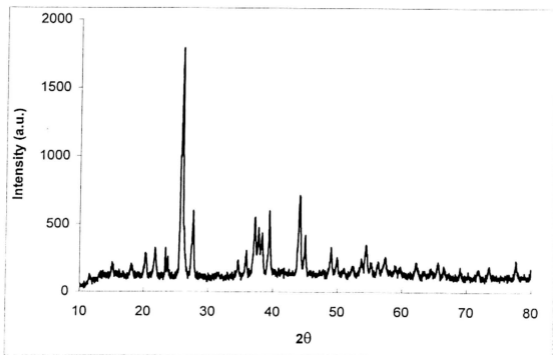


Figure 4.1 : X-ray diffractogram of pure PVC

Figure 4.2 : X-ray diffractogram of  $\text{LiCF}_3\text{SO}_3$ Figure 4.3 : X-ray diffractogram of  $\text{LiBF}_4$

The x-ray patterns for PVC -  $\text{LiCF}_3\text{SO}_3$  complex and PVC -  $\text{LiBF}_4$  complex are shown in Figure 4.4 and 4.5 respectively.

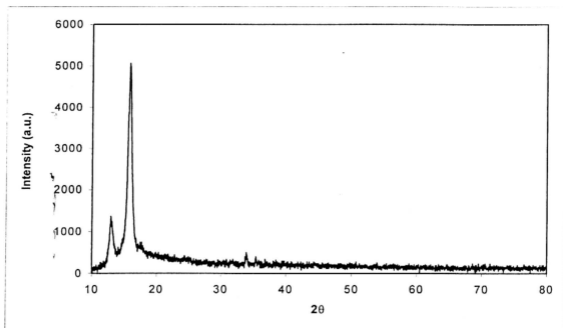


Figure 4.4 : X-ray diffractogram of PVC -  $\text{LiCF}_3\text{SO}_3$  complex

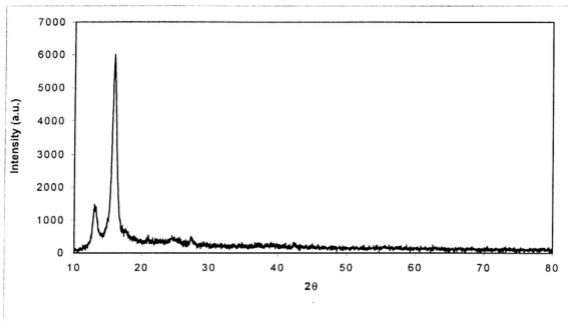


Figure 4.5 : X-ray diffractogram of PVC -  $\text{LiBF}_4$  complex

The incorporation of lithium salts into polymeric PVC matrices shows the disappearance of the diffraction peaks of salts and a shift in the PVC peaks to a  $2\theta$  angle of  $15.8^\circ$  and  $13.0^\circ$ . The absence of the characteristic diffraction lines of the lithium salts show that they are completely complexed by the polymer [150]. The appearance of shifted peaks shows evidence that complexation has occurred between the salts and the polymer.

Figure 4.6 to 4.10 shows the x-ray diffractogram complexes of  $[x \text{LiBF}_4 + (1-x) \text{LiCF}_3\text{SO}_3]$  [PVC] complexes with  $x=0.2, 0.4, 0.6, 0.7$  and  $0.8$  respectively.

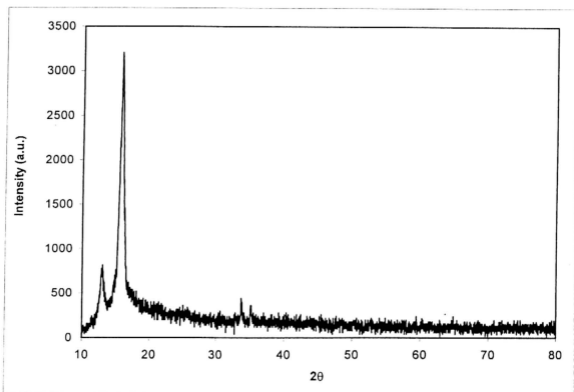


Figure 4.6 :  
X-ray diffractogram of  $[x \text{LiBF}_4 + (1-x) \text{LiCF}_3\text{SO}_3]$  [PVC] complex with  $x=0.2$

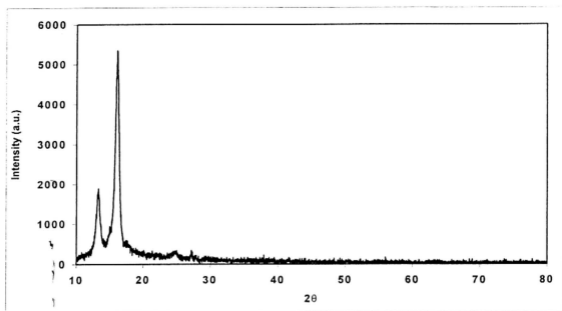


Figure 4.7 :  
X-ray diffractogram of  $[x \text{ LiBF}_4 + (1-x) \text{ LiCF}_3\text{SO}_3]$  [PVC] complex with  $x=0.4$

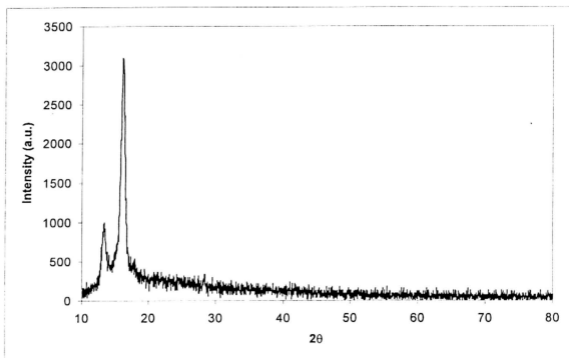


Figure 4.8 :  
X-ray diffractogram of  $[x \text{ LiBF}_4 + (1-x) \text{ LiCF}_3\text{SO}_3]$  [PVC] complex with  $x=0.6$

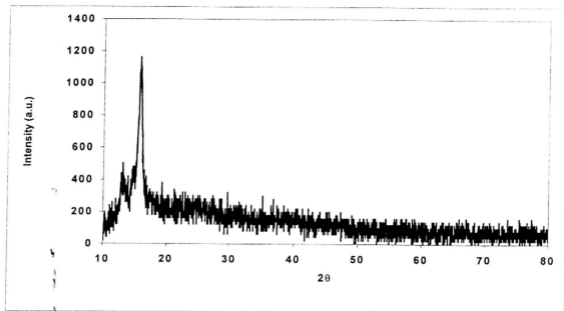


Figure 4.9 :  
X-ray diffractogram of  $[x \text{ LiBF}_4 + (1-x) \text{ LiCF}_3\text{SO}_3]$  [PVC] complex with  $x=0.7$

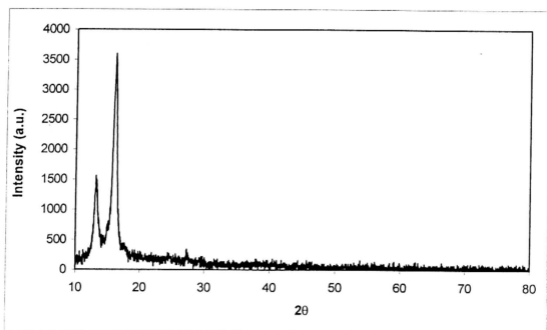


Figure 4.10 :  
X-ray diffractogram of  $[x \text{ LiBF}_4 + (1-x) \text{ LiCF}_3\text{SO}_3]$  [PVC] complex with  $x=0.8$

From the analysis, it is observed that there is a variation in relative intensity. Such changes in intensity confirms that the complexation takes place between PVC,  $\text{LiCF}_3\text{SO}_3$  and  $\text{LiBF}_4$  [151].

The intensity of the peaks corresponding to pure PVC in the above analysis has been found to decrease with the addition of the salts. This indicates the partial conversion of the crystalline phase in PVC to an amorphous phase [135].

For the above mixed salt system, XRD shows that the sample with  $x=0.7$  is the most amorphous sample. The amorphous/crystalline nature affects the electrical conductivity of the samples. These results are in corresponding agreement to the trend in conductivity value that was reported in chapter 3. From these diffractograms, the coherent or Scherrer Length was calculated using Scherrer equation and presented in Table 4.1 and in Fig.4.11. Coherent length measured using the peak at  $2\theta \approx 16^\circ$ .

x	Coherent length L <sub>c</sub> (Å)
0	14.14
0.2	14.21
0.4	13.96
0.6	13.42
0.7	13.28
0.8	13.44
1.0	13.78

Table 4.1 : Coherent length for  $[x \text{LiBF}_4 + (1-x) \text{LiCF}_3\text{SO}_3]$  [PVC] complex with various x values.



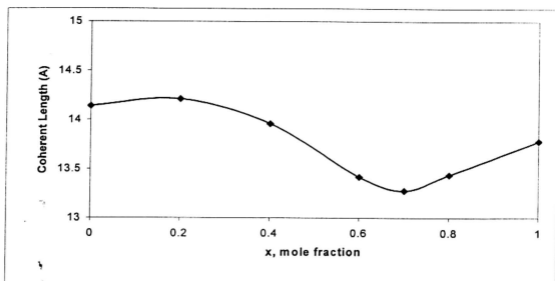


Figure 4.11 : Variation of coherent length as a function of mole fraction of  $\text{LiBF}_4$  in the  $[x \text{LiBF}_4 + (1-x) \text{LiCF}_3\text{SO}_3]$  [PVC] system.

Figure 4.11 shows that the sample with  $x=0.7$  has the smallest coherent length. Coherent length will decrease with increase in the amorphous nature of the sample. Figures 4.12 and 4.13 show the diffractogram of PVC- $\text{LiCF}_3\text{SO}_3$ - $\text{LiBF}_4$  complex which is plasticized with different amounts of ethylene carbonate (EC).

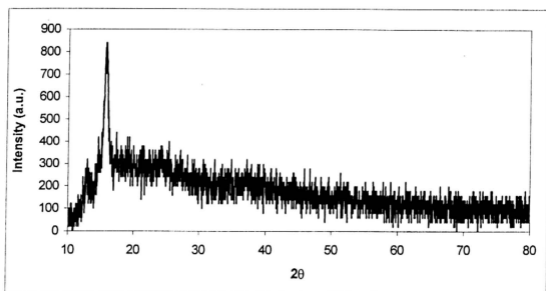


Figure 4.12 : Diffractogram of PVC - $\text{LiCF}_3\text{SO}_3$  -  $\text{LiBF}_4$  : EC (80:20)

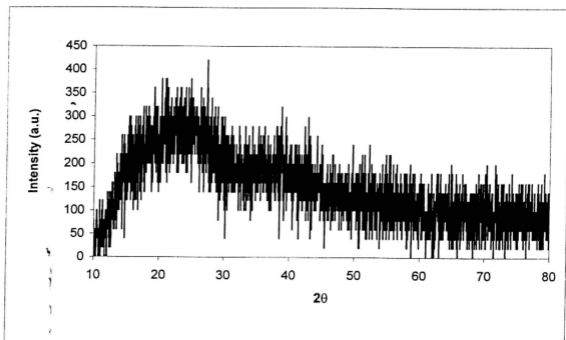


Figure 4.13 : Dffractogram of PVC - LiCF<sub>3</sub>SO<sub>3</sub> - LiBF<sub>4</sub> : EC (60 :40)

With the addition of 20 wt.% EC, the amorphous character of the sample is further increased and there is only one broad peak observed for the sample with 40 wt% of EC. This broad peak is called as the amorphous hump and is a typical characteristic of amorphous materials.

The diffractogram of PVC-LiCF<sub>3</sub>SO<sub>3</sub> -LiBF<sub>4</sub> -EC complex added with different amount of propylene carbonate is shown in Figures 4.14 and 4.15. It can be seen that PVC-LiCF<sub>3</sub>SO<sub>3</sub>-LiBF<sub>4</sub>-EC-PC complexes are highly amorphous. The amorphous nature produces greater ionic diffusivity in agreement with the high ionic conductivity that can be obtained in amorphous polymers having fully flexible backbones [83].

## 4.2 Thermal Studies

Thermal characterization of polymeric materials covers many aspects of material science. Thermal studies of the polymer electrolytes will provide us the information with regard to their thermal stability, crystallinity and other thermal parameters.

### 4.2.1 Differential Scanning Calorimetry (DSC)

Figure 4.16 shows the DSC thermogram of a pure poly (vinyl chloride) sample heated at a controlled rate. At the glass transition temperature,  $T_g$ , a small endothermic reaction is observed as the specific heat of the sample increases. As shown by the experiment, the recorded  $T_g$  for pure PVC is around  $54^\circ\text{C}$ . Beyond  $T_g$ , the plot appears as a small shifted baseline until an exothermic reaction becomes evident when the sample releases heat during crystallization. This crystallization peak,  $T_c$ , is close to  $162^\circ\text{C}$ . Upon further heating, the initial stage of another endothermic peak was observed at a temperature around  $280^\circ\text{C}$ . This is the melting point of pure PVC [41,118].

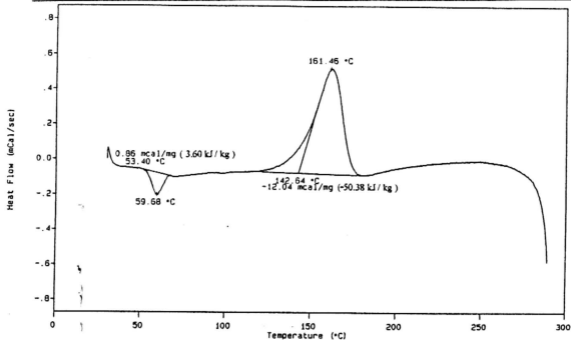
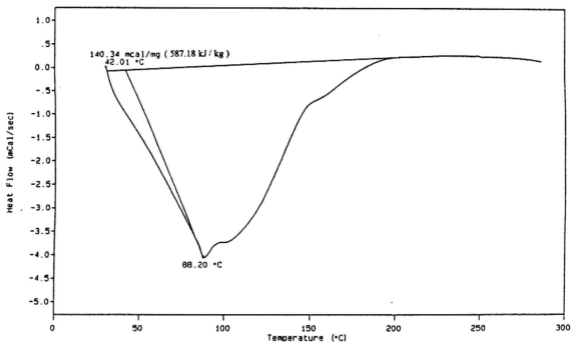


Figure 4.16 : DSC thermogram of pure PVC

The DSC thermogram of PVC-LiCF<sub>3</sub>SO<sub>3</sub> complex and the PVC-LiBF<sub>4</sub> complex are shown in Figure 4.17 and 4.18 respectively.

Figure 4.17 : DSC thermogram of PVC - LiCF<sub>3</sub>SO<sub>3</sub> complex

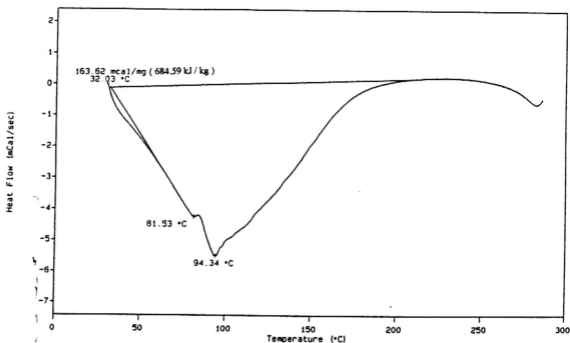


Figure 4.18: DSC thermogram of PVC - LiBF<sub>4</sub> complex

Results show that the glass transition of the PVC - salt complex is shifted towards higher temperatures relating to PVC, as expected, due to the lower degree of chain movements caused by chlorine co-ordination. The cation-chlorine binding energy, which is the driving force for salt dissolution, contributes to the increase in the barrier to rotation of the polymer segments. This is evidenced by a marked increase in glass transition temperature for PVC - salt complexes [73,78]. From the figures, we know that the  $T_g$  for PVC - LiCF<sub>3</sub>SO<sub>3</sub> complex and PVC - LiBF<sub>4</sub> complex are 65°C and 82°C respectively.

Figure 4.19 shows the DSC thermogram of  $[x\text{LiBF}_4 + (1-x)\text{LiCF}_3\text{SO}_3]$  [PVC] complex with  $x = 0.7$ . The value of glass transition temperature is around  $73^\circ\text{C}$ . This result shows that the  $T_g$  value of mixed salt system lies between the single salt system.

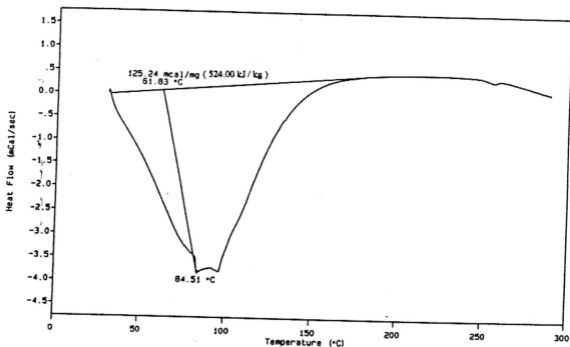


Figure 4.19 : DSC thermogram of  $[x \text{LiBF}_4 + (1-x) \text{LiCF}_3\text{SO}_3]$  [PVC] complex with  $x = 0.7$ .

The above results show that  $T_g$  varies from  $65^\circ\text{C}$  for  $\text{LiCF}_3\text{SO}_3$ [PVC] to  $82^\circ\text{C}$  in the case of  $\text{LiBF}_4$ [PVC]. Since the glass transition involves the freezing of large-scale molecular motions without a change in structure or the evolution of latent heat, one can conclude that both  $\text{LiCF}_3\text{SO}_3$  and  $\text{LiBF}_4$  decrease local chain mobility with  $\text{LiBF}_4$  having stronger influence [127].

The crystallization peak and melting peak have shifted to higher temperature level. Thus, these two peaks are not shown in the figures. This increase in crystallization

and melting temperature may be attributed to the increase in glass transition temperature of the polymer electrolyte.

PVC -  $\text{LiCF}_3\text{SO}_3$  and PVC -  $\text{LiBF}_4$  complexes have specific heat capacity of 140.34 mcal / mg and 163.62 mcal / mg respectively. The mixed salt system shows a value of 125.24 mcal / mg. This reduced heat capacity of the mixed salt system means that the crystallinity is reduced [152].

The DSC thermogram for the plasticized PVC- $\text{LiCF}_3\text{SO}_3$ - $\text{LiBF}_4$  polymer electrolyte based on ethylene carbonate is shown in Figure 4.20.

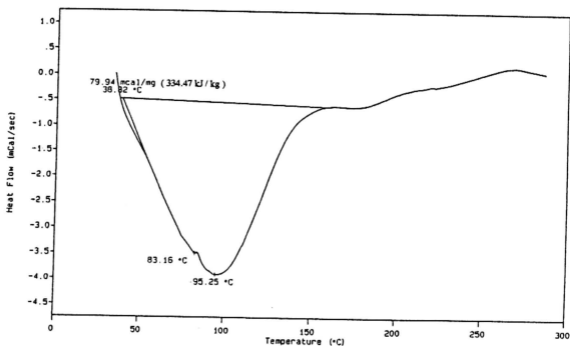


Figure 4.20 : DSC thermogram of PVC -  $\text{LiCF}_3\text{SO}_3$  -  $\text{LiBF}_4$  - EC system

The  $T_g$  and specific heat capacity which are calculated from Figure 4.20 are  $61^\circ\text{C}$  and 79.94 mcal / mg. Plasticized samples present lower value of  $T_g$  than the

plasticizer free samples due to its lubricating effect [78]. Usually, the plasticizer behaves like a solvent when mixed with a polymer and results in the lowering of the glass transition temperature. This lowered  $T_g$  also confirms the PVC plasticization effect. The plasticization effect is related to weakening of the dipole-dipole interactions due to the presence of the plasticizer molecules between the PVC chains [48]. The reduced heat capacity shows that the crystallinity is also reduced.

#### 4.2.2 Thermogravimetric Analysis (TGA)

Thermogravimetric analysis will give information regarding the thermal stability of the polymer electrolyte with increasing temperature. The weight loss which is obtained from the TGA graphs will be used to study the thermal stability of the polymer electrolytes.

The thermogravimetric curve obtained with pure PVC film is shown in Figure 4.21. The TGA curve shows a small weight loss at around 100°C. This may be due to the transition peak of the polymer electrolyte sample. The second weight loss can be observed at a temperature of around 160°C. This is due to the crystallization peak of the sample. This result is confirmed by the DSC studies.



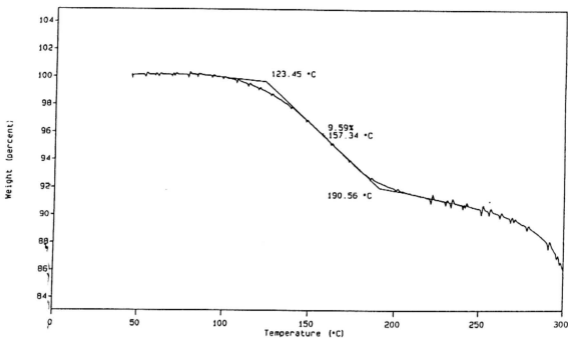
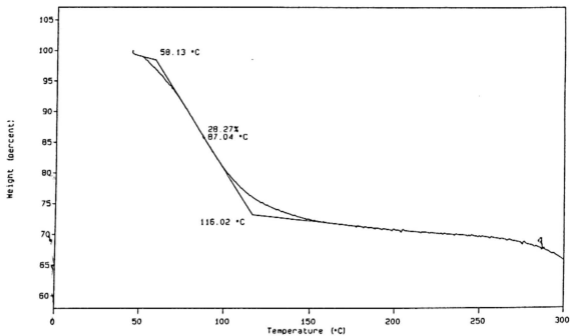
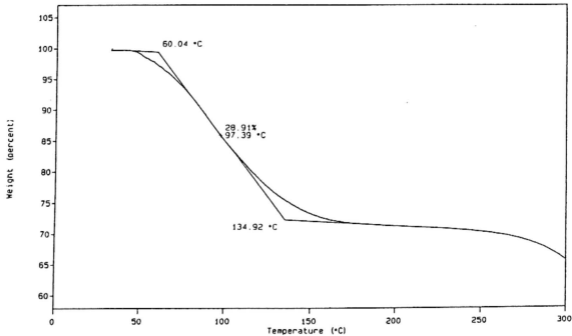


Figure 4.21 : Thermogravimetric curve for pure PVC film.

Figure 4.22 and 4.23 shows the TGA traces for PVC -  $\text{LiCF}_3\text{SO}_3$  complex and PVC-  $\text{LiBF}_4$  complex respectively. Both the samples began to lose mass at temperature below  $100^\circ\text{C}$ . This initial loss results from residual solvent evaporation and the transition of the polymer electrolyte sample. Volatilization of monomers and oligomers adsorbed in the matrix can also be responsible for this initial mass loss [50]. The percentage weight loss for PVC -  $\text{LiCF}_3\text{SO}_3$  complex is 28.27% and for the PVC- $\text{LiBF}_4$  complex is 28.91%. These results confirm that both complexes have approximately the same thermal stability. The second weight loss begins at a temperature of above  $250^\circ\text{C}$ . This may be due to the crystallization of the above polymer electrolyte samples. This increase in temperature of second weight loss is due to the increase in  $T_g$  values.

Figure 4.22 : Thermogravimetric trace for PVC - LiCF<sub>3</sub>SO<sub>3</sub> complexFigure 4.23 : Thermogravimetric trace for PVC - LiBF<sub>4</sub> complex.

The TGA curve of mixed  $\text{LiCF}_3\text{SO}_3 / \text{LiBF}_4$  electrolytes :  $[\text{xLiBF}_4 + (1-\text{x})\text{LiCF}_3\text{SO}_3]$  [PVC] complex with  $x = 0.7$  is shown in Figure 4.24. From the curve, we can observe that the temperature of the first weight loss and second weight loss is approximately around the same value. The same argument holds for these two weight losses. However, the percentage weight loss for the mixed salt system is reduced to 24.40%. This indicates that the mixed salt system has better thermal stability than the single salt system [123].

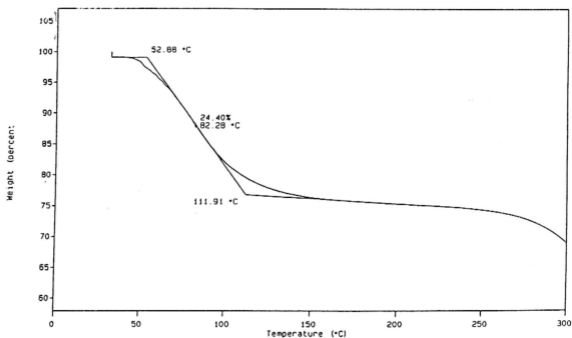


Figure 4.24 : Thermogravimetric curve for PVC -  $\text{LiCF}_3\text{SO}_3$  -  $\text{LiBF}_4$  complex

The TGA plot of PVC- $\text{LiCF}_3\text{SO}_3$ - $\text{LiBF}_4$  complex which was plasticized with ethylene carbonate (EC) is shown in Figure 4.25. This plasticized film shows a weight loss of 19.95% at a temperature below 100°C. From this it is clear that the polymer

electrolyte containing EC has more thermal stability than the unplasticized polymer electrolytes in the present study.

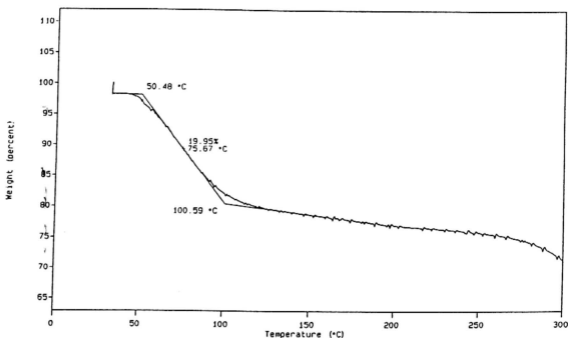


Figure 4.25 : Thermogravimetric plot for PVC - LiCF<sub>3</sub>SO<sub>3</sub> - LiBF<sub>4</sub> - EC complex.

Figure 4.26 shows the TGA curve of double plasticizer complex. The additional plasticizer used in this study is propylene carbonate (PC). The composition of this complex is PVC : LiCF<sub>3</sub>SO<sub>3</sub> - LiBF<sub>4</sub> : EC - PC = 15 : 15 : 70.

From the figure obtained, we can observe 6.70% weight loss at a temperature below 100°C and 27.83% weight loss at a temperature around 150°C. The second weight loss, as explained earlier is because of the crystallization of the polymer electrolyte. This figure also indicates that the crystallization temperature is decreased

compared to the earlier complexes. This may be due to the decrease in glass transition temperature with respect to increase in plasticizer content. The thermal stability of the polymer electrolyte also decreases with the increase in plasticizer content. This is because in the region between 100°C and 150°C a higher weight loss of 27.83% is observed compared to the weight loss of 9.59% for the pure PVC sample.

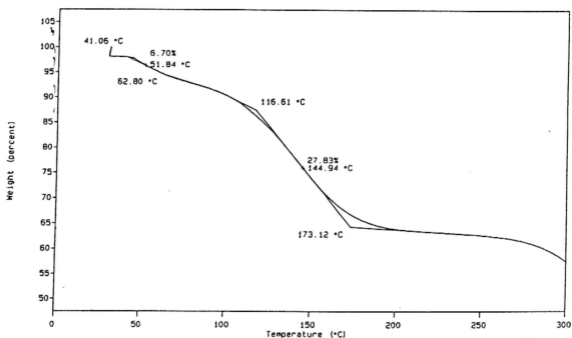


Figure 4.26 : Thermogravimetric plot for double plasticizer system.